

Development and Validation of an Air Spring Multiphysical Model

F. Renno, S. Strano, M. Terzo

Abstract—This paper presents a multiphysical model of a reversible sleeve air spring to be employed for design and simulation purpose. A multiphysical approach, combining fluid flow with solid mechanics, has been considered to study the interaction between the fluid and the solid structure of the air spring under different pressure conditions. Experimental tests have been developed applying several compression loads to the air spring and measuring the deformation and the reaction force for different values of the initial pressure. An experimental validation has been executed analyzing and comparing the mechanical behaviour of the actual prototype and the virtual model. In particular, the 3D deformation of the air spring has been acquired by means of the Reverse Engineering techniques and the results have been compared with the simulated ones. Moreover, the experimental and simulated air spring vertical stiffness have been matched in order to verify the accuracy of the multiphysical model. The validation procedure demonstrated that the simulation results fitted the experimental ones for different testing conditions.

Index Terms— Air Spring, Multiphysics, CFD, Structural Analysis, Reverse Engineering, FEM, Elastomers, Mooney-Rivlin model

I. INTRODUCTION

PNEUMATIC components, such as air springs, have long been used as vibration isolation and levelling devices. They are typically used when a higher spring rate in a smaller package than can be provided by an equivalent steel spring is required. Moreover, they represent a valid solution for load levelling functions by adding or removing air. Air Springs (AS) can be found in many types of vehicles, such as automobiles, railway vehicles, buses, construction and agricultural vehicles for which active and semi-active vibration control systems are often adopted [1-2]. In large truck applications, AS can be used for cab and seat suspensions in addition to truck and trailer chassis suspensions. An accurate air spring model represents a tool functional to simulate and analyze the characteristics of air springs under different load conditions and when they are equipped in complex multibody systems [3-5]. Various attempts have been done to build a more accurate model. A nonlinear one dimensional air spring model, used for railway

vehicles, was proposed by Berg [6, 7]. The empirical formulas of various air springs [8-10] can be deduced by means of a graphical method and related assumptions. But, the accuracy of this method is too low due to the complex geometry, the structure and the material. Currently, the stiffness of an air spring is obtained mostly through experiments. In recent years, several approaches [11-13] have been used to analyze air springs [14]. Starting from them, a Finite Element (FE) method to develop a new AS model and a double validation procedure has been utilized and described in this paper. The first has been a “geometrical validation” carried out by means of a Reverse Engineering (RE) procedure. The second has been an “experimental validation” performed with reference to the vertical stiffness of the air spring.

Main target was to obtain an accurate Digital Mock-Up (DMU) to be used in virtual environments to set and perform multiphysical analyses. The Virtual Prototyping (VP) techniques allow to create realistic and helpful models for many types of simulations. Therefore, they are used in a lot of fields such as computer graphics (videogames and renderings), industrial, educational and medical. In the last years, they are becoming very important for the design and the development of the nuclear fusion plants [15-25]. One of the most important among the VP techniques is the CAD modeling that makes it easy to generate the leading actor for each kind of simulation i.e. a virtual model characterized by physical and mechanical properties. When it is not possible to count on the original CAD model the RE techniques allow to acquire the shapes of 3D objects and reconstruct them in digital format. If their successive modification is needed (i.e. to perform FEM analyses and optimizations), a complex feature recognition phase, not free from errors, is required [10]. According to the targets (i.e. quickness, precision, low costs) it is possible to use contact or contactless systems.

So, the shape of a real air spring has been acquired, reconstructed and matched with the FE model developed to detect differences and similarities. Successively, the force-displacement curves have been compared.

II. CASE STUDY

A. Air Spring Description

Air springs are designed and manufactured in various shapes and sizes to meet a wide variety of applications. Two common types are the convoluted or bellows and the reversible sleeve or rolling lobe. A convoluted air spring contains one or more lobes. A reversible sleeve type air spring contains a piston on which the elastomeric material

Manuscript received September 13, 2016; revised January 31, 2017.

F. Renno is with the *Department of Industrial Engineering, University of Naples Federico II*, Napoli, 80125 ITALY (e-mail: fabrizio.renno@unina.it).

S. Strano is with the *Department of Industrial Engineering, University of Naples Federico II*, Napoli, 80125 ITALY (e-mail: salvatore.strano@unina.it).

M. Terzo is with the *Department of Industrial Engineering, University of Naples Federico II*, Napoli, 80125 ITALY (corresponding author, phone +390817683277; fax +390812394165; e-mail: mario.terzo@unina.it).

moves as the height of the air spring changes in relation to load variations. In this work, a reversible sleeve air spring has been considered for the multiphysical analysis.

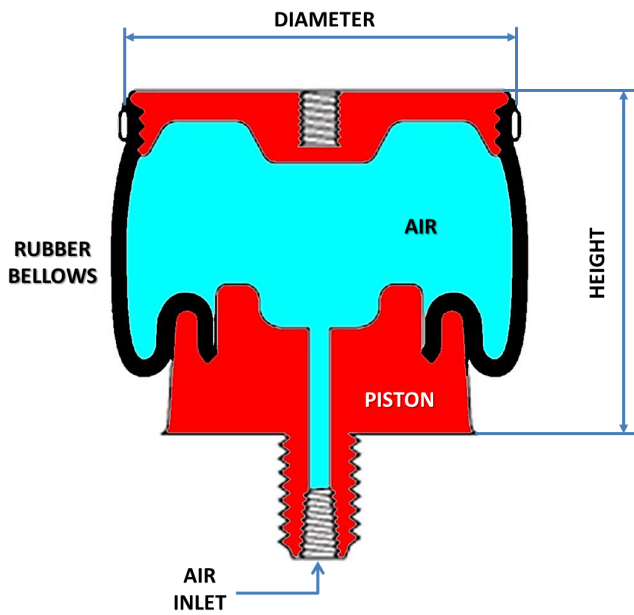


Fig. 1. Air Spring scheme.

B. CFD and Multiphysical Approach

Computational Fluid Dynamics (CFD) allows to analyze and, in some cases, solve problems that involve fluid flows. It is used to simulate the interaction between liquids and gases with surfaces by means of the definition of adequate boundary conditions [26, 27]. The motion of fluids is ruled by the Navier-Stokes equations (1). They link the fluid viscosity (\mathbf{u}), the fluid pressure (p), the fluid density (ρ), and the fluid dynamic viscosity (μ). The Navier-Stokes equations were derived by Navier, Poisson, Saint-Venant, and Stokes between 1827 and 1845 [28]. These equations are always solved together with the continuity equation (2).

$$\rho \left(\frac{\partial \mathbf{u}}{\partial t} + \mathbf{u} \cdot \nabla \mathbf{u} \right) = -\nabla p + \nabla \cdot (\mu (\nabla \mathbf{u} + (\nabla \mathbf{u})^T)) - \frac{2}{3} \mu (\nabla \cdot \mathbf{u}) \mathbf{I} + \mathbf{F} \quad (1)$$

$$\frac{\partial \rho}{\partial t} + \nabla \cdot (\rho \mathbf{u}) = 0 \quad (2)$$

The Navier-Stokes equations represent the conservation of momentum, whereas the continuity equation represents the conservation of mass. The solution of these equations (if possible) for a particular set of boundary conditions (such as inlets, outlets, and walls) predicts the fluid velocity and its pressure in a given geometry. Because of their complexity, they only admit a limited number of analytical solutions. However, several hypotheses on the compressibility or the turbulence of flow can be assumed to simplify these equations [26, 27]. For instance, when the Mach number is very low, it is possible to assume that the flow is incompressible i.e. the density is assumed to be constant and the continuity equation becomes $\nabla \cdot \mathbf{u} = 0$. Otherwise, for more complex geometries it is needed to solve it numerically. Besides, when it is necessary to consider the deformations that a fluid can cause on an elastic structure,

multiphysical analyses can provide very interesting results. A typical approach is based firstly on the computation of the loads generated by the fluid and then to its application to the elastic structure to determine its deformation. Otherwise, the Fluid-Structure Interaction (FSI) study combines the laws of fluid dynamics and structural mechanics allowing to study the bi-directional influences between the fluid and the object. So, when a structure is subject to a fluid flow, it can be deformed by the stresses and strains generated. The extension of these deformations, that depends on the pressure and on the velocity of the flow, can be quite small or in some cases very large [26, 27]. Besides, the material used for the structure can strongly affect the results. In fact, if it is characterized by a hyperelastic behaviour large deformations are to be considered. Furthermore, it is possible to analyze and define the effects of the deformations of the structure on the fluid in order to complete the evaluation of the behaviour of the whole system.

III. CAD AND MULTIPHYSICAL MODELLING OF THE AIR SPRING

A. RE of the Case Study

Starting point of the process was the 3D acquisition of the air spring used as case study at atmospheric pressure to get the original shape in a file format compatible with the CAD and multiphysical environments. Thus, a set of laser acquisitions was realized and the 3D CAD model of the air spring was obtained (Fig.2).

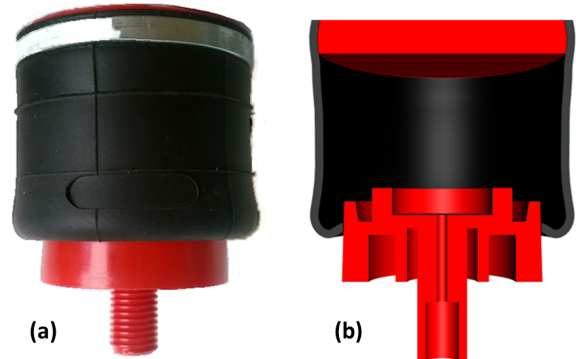


Fig. 2. Original (a) and reconstructed (b) models of the Air Spring used as case study.

The system used for the RE process is a low-cost laser scanner but it guaranteed the accuracy (± 0.5 mm) and the resolution (0.9 mm) needed for the comparison of the results obtained in different load conditions.

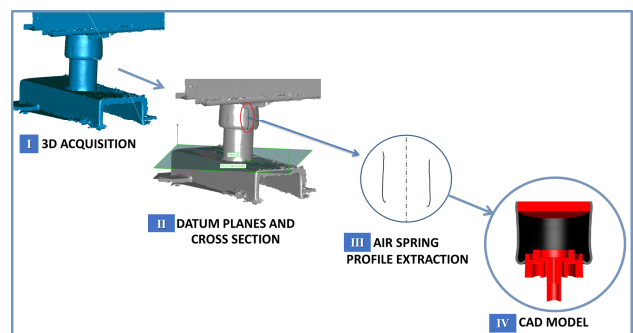


Fig. 3. RE process for the reconstruction of the 3D model of the Air Spring.

According to a typical RE process, after the digitizing phase the point clouds were imported in a RE dedicated software. The tessellated model was created and successively NURBS surfaces were used to properly fit the acquired point clouds. So, it was possible to create an accurate skin of the air spring and then to define the needed references (points, axes and datum planes) to extract the curves related to the profile of the rubber bellows. In this way, the CAD model of the air spring was created counting on accurate guide lines for the sketch phase and for the successive solid modelling step (Fig. 3). Particularly detailed was the reconstruction of the rubber bellows. In fact, the correct analysis of the results was based on the comparison between the original profile and the deformed ones. This approach allowed to get a very realistic shape of the rubber bellows (without approximations) and to improve the CAD and, especially, the multiphysical modelling.

B. Multiphysical Model

A multiphysical approach, combining fluid flow with solid mechanics, was considered to study the interaction between the fluid and the solid structure of an air spring suspension under different pressure conditions (Fluid-Structure Interaction). Main target was to define how a fluid (air) flow can deform the rubber bellows. The use of the arbitrary Lagrangian-Eulerian (ALE) technique allows to solve the problem for the flow in a continuously deforming geometry. The fluid flow was formulated by means of an Eulerian description, whereas the other components (studied with solid mechanics), in particular the rubber bellows, were expressed starting from a Lagrangian description [26]. To simplify the problem a Single-phase Newtonian fluid and an incompressible flow were considered. So, the fluid flow was described by the incompressible Navier-Stokes equations for the velocity field, $\mathbf{u} = (u, v)$, and the pressure p in the spatial (deformed) moving coordinate system:

$$\rho \frac{\partial \mathbf{u}}{\partial t} - \nabla \cdot [-p\mathbf{I} + \eta(\nabla \mathbf{u} + (\nabla \mathbf{u})^T)] + \rho((\mathbf{u} - \mathbf{u}_m) \cdot \nabla) \mathbf{u} = \mathbf{F} \quad (3)$$

$$-\nabla \cdot \mathbf{u} = 0 \quad (4)$$

In these equations, \mathbf{I} is the unit diagonal matrix and \mathbf{F} is the volume force affecting the fluid. $\mathbf{F}=0$ because no gravitation or other volume forces on the fluid were considered. The coordinate system velocity is $\mathbf{u}_m = (u_m, v_m)$. The ALE method handles the dynamics of the deforming geometry and the moving boundaries with a moving grid. New mesh coordinates are computed on the area based on the movement of the structure's boundaries and mesh smoothing [26]. The Navier-Stokes equations that solve the flow are formulated for these moving coordinates. The structural mechanics portion of the model does not require the ALE method, and it is solved in a fixed coordinate system as usual. The structural deformations are solved by means of elastic and nonlinear geometry formulations to allow large deformations [26]. All the object boundaries are subject to a load from the fluid given by:

$$\mathbf{F}_T = -\mathbf{n} \cdot (-p\mathbf{I} + \eta(\nabla \mathbf{u} + (\nabla \mathbf{u})^T)) \quad (5)$$

where \mathbf{n} is the normal vector to the boundary. This load represents a sum of pressure and viscous forces. So, the Navier-Stokes equations are solved on a freely moving deformed mesh, which constitutes the fluid domain. The deformation of this mesh relative to the initial shape of the domain is computed by means of the Winslow smoothing [26].

Therefore, the Fluid-Structure Interaction (FSI) module of the COMSOL Multiphysics software was used to determine numerically the deformation of the rubber bellows of the air spring, and then to compare it to the experimental solution given by the RE techniques. A multiphysical model was realized assuming a steady state study.

The CAD model created by means of the RE acquisitions was imported into the COMSOL environment. Afterwards, the selection of the materials was very important. For the base and the top parts of the air spring, plastic was set and the elastic behaviour was considered. As the rubber bellows of the air spring is typically an elastomer and is subjected to large deformations, a hyperelastic behaviour was simulated for it according to the Mooney-Rivlin model (two parameters) that is recommended in case of AS suspensions. This kind of model describes the material's stress-strain relationship as a function of two empirically determined constants. The knowledge of the Mooney-Rivlin constants for a material is very important to perform finite element modelling of elastomers. However, the determination of these constants requires biaxial deformation of the material and a measurement system to evaluate stress and strain in this configuration [26].

Hyperelastic constitutive laws are recommended for model materials that respond elastically when subjected to very large strains. They are mainly used to model rubber-like behaviour of polymers and foams subjected to reversible deformations. Typical examples include rubber seals and elastomer parts of shock and vibration control systems [27, 30] whose mathematical model are usually validated by means of suitable experimental test rig [31-35].

The Navier-Stokes equations are characterized by a non-linear term that is responsible for the transfer of kinetic energy to the turbulent cascade. Only in some cases, such as for the one-dimensional flow, they can be reduced to linear equations. The nonlinearity, most of the time, causes the difficulty or the impossibility to solve these equations. For instance, even very small variations of pressure can determine the "explosion" of the solution. In these cases, the convergence is not possible. To try to avoid this problem it is recommended to set up the multiphysics model adequately, i.e. to build regular and detailed meshes, to use appropriate solvers, to define the boundary conditions properly and to choose the most suitable method to describe and study the (elastic and hyperelastic) behaviour of the materials.

So, the meshes realized in the COMSOL environment (Fig. 4(b)) were optimized and refined for fluid dynamic problems.

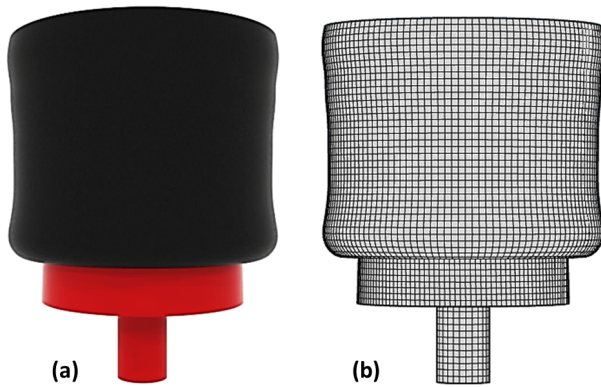


Fig. 4. CAD model (a) and 3D mesh (b) of the Air Spring.

C. Multiphysical Analysis Results

Hereafter three kind of models are described and used for the cases studied:

- the (initial) “CAD model” i.e. the Digital Mock-Up of the air spring;
- the “RE models” reconstructed by means of RE processes starting from the acquisition of the air spring deformed under different load conditions;
- the “FEM models” obtained thanks to the multiphysics approach defined in the COMSOL environment.

The CAD model described in the previous paragraph was used to study the behaviour of the air spring under different boundary conditions. It allowed to evaluate the von Mises stresses and to determine the max deformation of the rubber bellows at $p = 2, 3, 4$ bar respectively (Figs. 5-7).

At $p = 2$ bar there was the 0.9635 mm max deformation depicted in Fig. 5. The black line shows the inner profile of the (initial) CAD model of the rubber bellows used for the analyses in the COMSOL environment.

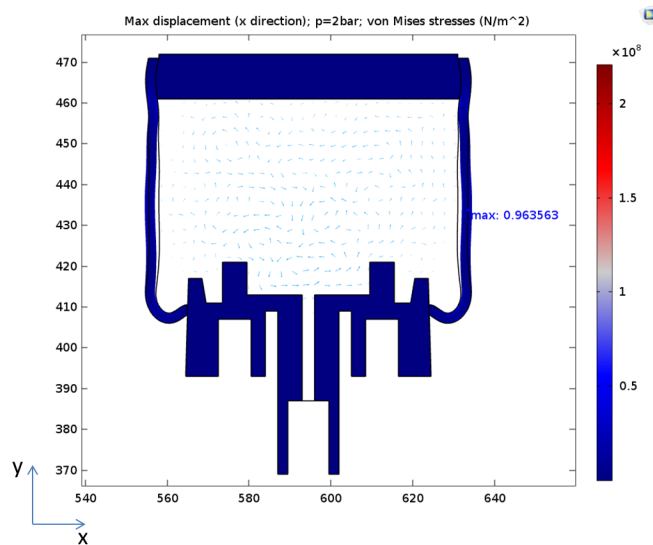


Fig. 5. Max displacement in x direction at $p = 2$ bar. Numerical result by COMSOL multiphysics software. Shape deformation of the rubber bellows evaluated respect to the CAD model of the Air Spring.

At $p = 3$ bar the 1.3784 max deformation shown in Fig. 6 was detected.

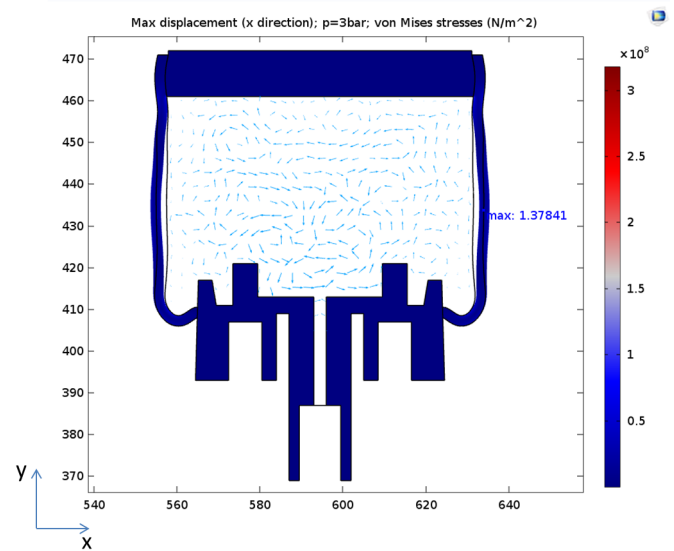


Fig. 6. Max displacement in x direction at $p = 3$ bar. Numerical result by COMSOL multiphysics software. Shape deformation of the rubber bellows evaluated respect to the CAD model of the Air Spring.

At $p = 4$ bar the 1.7517 max deformation shown in Fig. 7 was detected. These values, calculated thanks to the numerical approach followed in COMSOL multiphysics software, will be then compared to the measurements of the real profile of the air spring done by means of the RE techniques to validate the results obtained.

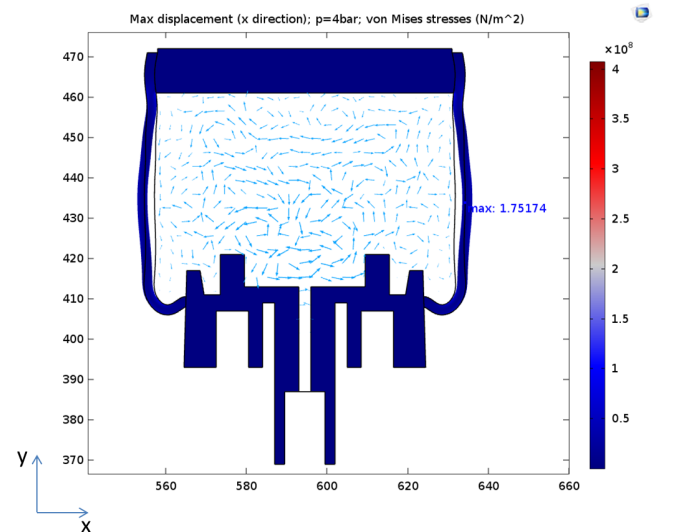


Fig. 7. Max displacement in x direction at $p = 4$ bar. Numerical result by COMSOL multiphysics software. Shape deformation of the rubber bellows evaluated respect to the CAD model of the Air Spring.

IV. MODEL VALIDATION AND RESULTS

A. Test Bench Description

Experimental tests have been developed with a specific test bench that has allowed to apply a compression load to the air spring, by measuring the deformation and the force for different values of the initial pressure. Fig. 8 shows the air spring (detailed view in Fig. 9), the hydraulic actuator and the load cell for the compression force measurement. An air compressor has been used for the initial pressure regulation.

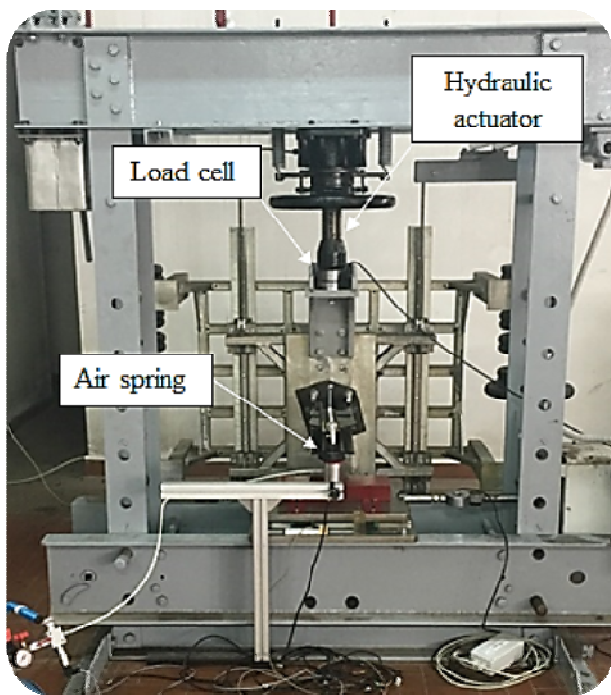


Fig. 8. Test rig realized for the experimental analyses.



Fig. 9. Detailed view of the test rig realized for the experimental analyses.

B. Evaluation of the deformation of the Rubber Bellows by means of RE techniques

Three main analyses were set up. Starting from different load conditions ($p = 2, 3, 4 \text{ bar}$) the deformation of the rubber bellows was acquired by means of the RE techniques. The top and the bottom parts of the air spring were constrained to the test rig in order to have an assigned distance between it. The use of a portable laser scan allowed to reach each zone of interest with an acceptable accuracy.

Fig. 10(a) shows the real profile of the air spring ($p = 4 \text{ bar}$). Fig. 10(b) presents its deformed shape acquired by means of the RE techniques. So, the measurement of the deformation of the rubber bellows for different load conditions allowed to obtain very accurate data for the successive comparison with the numerical results given by the multiphysical analysis.

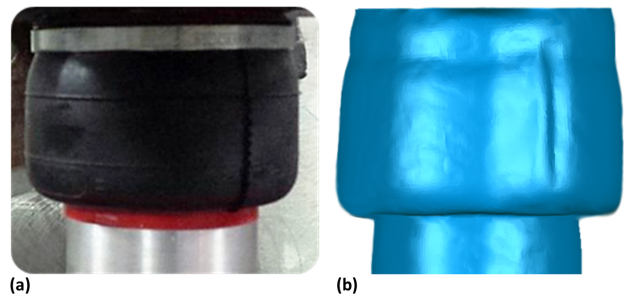


Fig. 10. Comparison between the real profile (a) of the air spring and the model reconstructed (b) by means of the RE techniques.

To validate the procedure ideated the comparison between the original shape (CAD model) of the rubber bellows and the deformed profile was needed. The top and the bottom part of the air spring on the test rig were constrained in order to avoid their displacements in x, y, z directions and to evaluate the “pure” deformation of the rubber bellows under different load conditions. So, firstly the RE techniques were used to digitalize the shape of the air spring without loads on it except the atmospheric pressure (starting conditions), and then to measure the deformation of the rubber bellows under different load conditions (2, 3 and 4 bar). Afterwards, the RE models were realized and the starting profile and the reconstructed one were imported into the CAD environment to calculate the distance between them. As an example, the max distance evaluated by means of Rhinoceros software between the reconstructed curve (blue) of the external profile of the air spring and the original one (black) is shown in Fig. 11, considering the $p = 4 \text{ bar}$ loading condition. So, it was possible to estimate the max deformation value (2.0979 mm) of the rubber bellows in the x direction (Fig. 11).

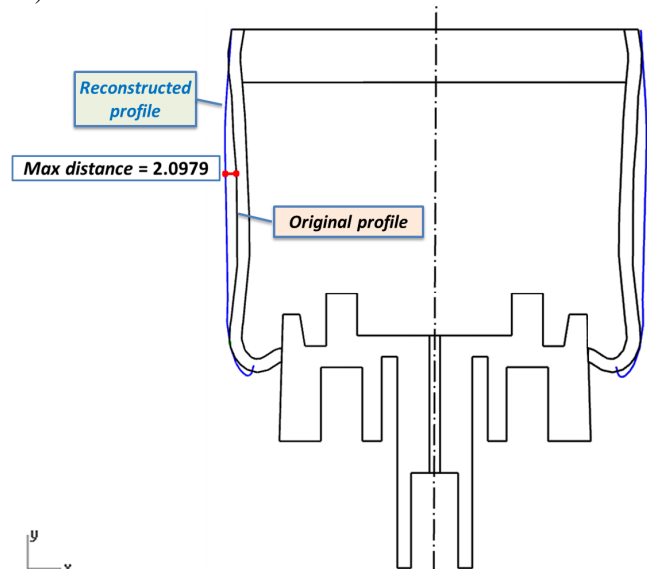


Fig. 11. Comparison realized in CAD environment between the reconstructed curve (blue line) of the real profile of the air spring ($p = 4 \text{ bar}$) and the original one.

Furthermore, the 3D comparison between the results of the FEM analyses and the models reconstructed by means of the Reverse Engineering techniques was realized to complete the study. Fig. 12 shows the 3D models of the configuration measured by means of the RE techniques and

the FEM model obtained thanks to the multiphysics approach. The 3D check allows to analyze the deviation between the Measured Data and the Reference (gray model), i.e. the FEM results, by projecting all paired points (point clouds obtained by means of the RE process) onto the Reference Data. So, the deviation is displayed with a color map which helps to detect negative and positive peaks.

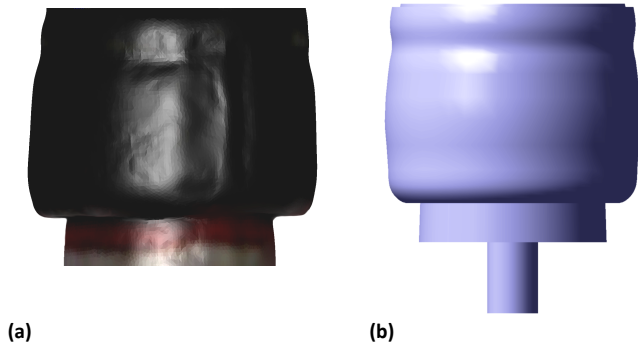


Fig.12. “RE model” and “FEM model” used for the comparison between the “measured” and the “calculated” geometries at the $p = 4 \text{ bar}$ pressure condition.

Fig. 13 shows the distances between the entities of the “FEM model” (gray) and of the “RE model” by means of colours at the $p = 4 \text{ bar}$ condition. The detected gaps are acceptable in terms of similarity of shapes and values calculated and measured respectively, demonstrating the validity of the procedure adopted and of the starting hypotheses.

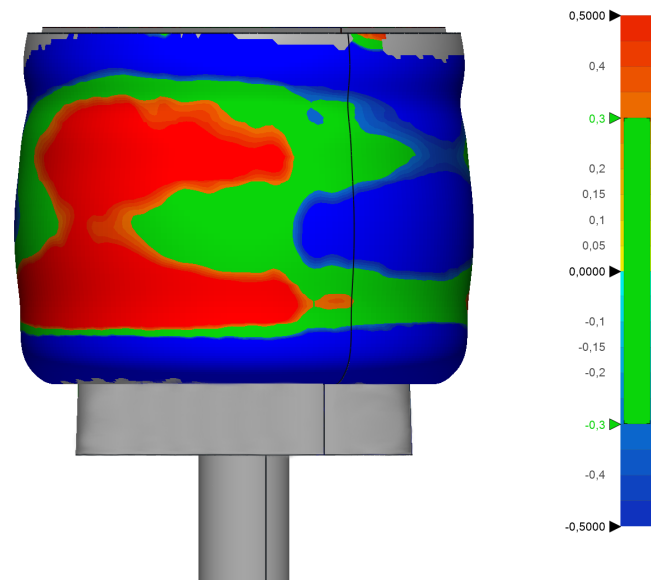


Fig. 13. Comparison realized in CAD environment between the FEM model (gray) and the “RE model” of the air spring at $p = 4 \text{ bar}$.

Similar results were obtained for the other pressure conditions (2 and 3 bar) but for the sake of simplicity only the outcomes obtained at $p = 4 \text{ bar}$ are shown.

C. Validation of Vertical Stiffness

The experimental measurements for the validation of the air spring vertical stiffness provided by the numerical model have been obtained with a load cell positioned between the

spring and the hydraulic actuator, a displacement sensor and a pressure sensor for the air spring internal pressure measurement. The simulated and experimental vertical stiffness of the air spring have been compared in order to verify the accuracy of the model. In particular, the model validation has been realized considering the vertical static stiffness, which represents the spring behaviour under static load. Figs. 14-16 show the force-displacement curves of the air spring obtained under different given initial air pressures. In these curves, the tangential direction in each point represents the corresponding vertical stiffness of the corresponding displacement. The spring is compressed in the range [45, 95] mm.

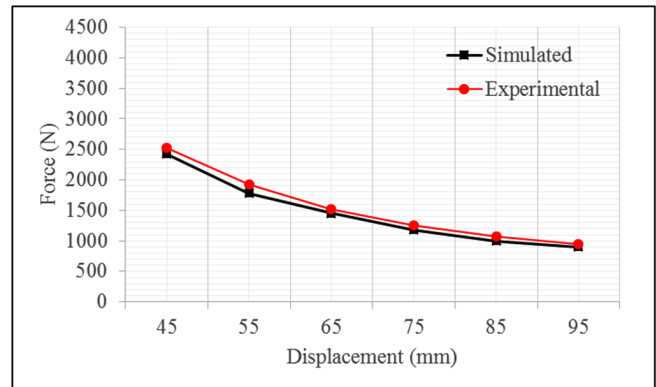


Fig. 14. Comparison of vertical stiffness (initial air pressure = 2 bar).

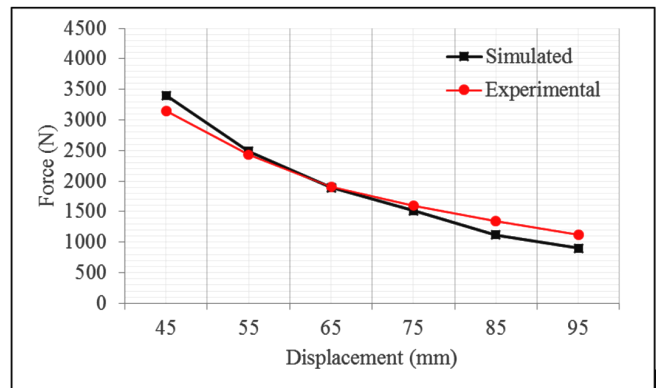


Fig. 15. Comparison of vertical stiffness (initial air pressure = 3 bar).

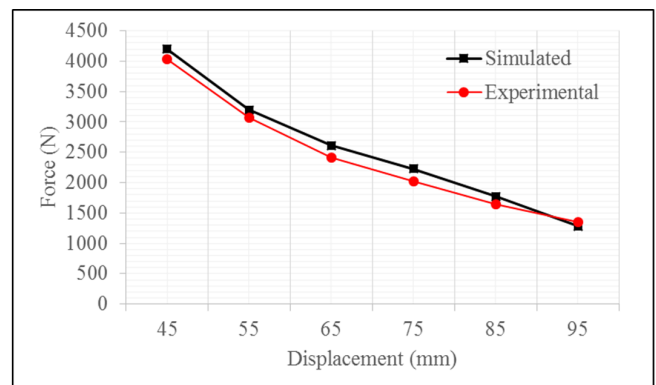


Fig. 16. Comparison of vertical stiffness (initial air pressure = 4 bar).

The simulated results of Figs. 14-16 illustrate that the numerical model approximately fits the experimental results in all the given strokes and initial air pressures. Indeed, under all the given initial air pressures, the trend of the numerical model is generally consistent with the experiment results. The differences between the numerical force-

displacement curves and the experimental ones are higher for the 4-bar initial pressure. This error could be due to geometric nonlinearity, material nonlinearity and to some factors that have not been considered in the numerical model. Nevertheless, the vertical stiffness of the proposed numerical model has a good agreement with the experiment results.

V. CONCLUSION

A multiphysical model of an air spring has been realized to perform simulations in several conditions. A gas-solid coupling and the boundary definition have been considered in order to model the Fluid-Structure Interaction that represents a fundamental phenomenon in air spring. A validation procedure has been executed to show the performance of the proposed model, functional for predictive analysis and optimal design. In particular, it was possible thanks to the combined use of RE techniques and Multiphysics approach in order to perform meaningful comparisons between numerical and measured results.

REFERENCES

- [1] F. Renno, S. Strano, M. Terzo, "Air spring and magnetorheological damper: An integrated solution for vibration control," *Lecture Notes in Engineering and Computer Science*, 2218, pp. 945-950, 2015.
- [2] D. Guida, D. C. M. Pappalardo, "Control Design of an Active Suspension System for a Quarter-Car Model with Hysteresis," *Journal of Vibration Engineering and Technologies*, 3 (3), pp. 277-299, 2015.
- [3] C. M. Pappalardo, "A Natural Absolute Coordinate Formulation for the Kinematic and Dynamic Analysis of Rigid Multibody Systems," *Nonlinear Dynamics*, 81(4), pp. 1841-1869, 2015.
- [4] D. Guida, C. M. Pappalardo, "Forward and Inverse Dynamics of Nonholonomic Mechanical Systems," *Meccanica*, 49 (7), pp. 1547-1559, 2014.
- [5] C. M. Pappalardo, M. D. Patel, B. Tinsley, A. A. Shabana, "Contact Force Control in Multibody Pantograph/Catenary Systems," *Proceedings of the Institution of Mechanical Engineers, Part K: Journal of Multibody Dynamics*, 230 (4), pp. 307-328, 2016.
- [6] M. Berg, "A model for rubber springs in the dynamic analysis of rail vehicles," *Proceedings of the Institution of Mechanical Engineers, Part F: Journal of Rail and Rapid Transit.*, 211 (1997) 95-108.
- [7] M. Berg, "A nonlinear rubber spring model for rail vehicle dynamics analysis," *Vehicle System Dynamics*, 30 (1998) 197-212. H. Poor, *An Introduction to Signal Detection and Estimation*. New York: Springer-Verlag, 1985, ch. 4.
- [8] Z. Jianwen, Z. Dejun, L. Yi et al., "Survey of automotive air spring suspension system," *Journal of Highway and Transportation Research and Development*, no. 12, pp. 151-155, 2002 (Chinese).
- [9] Z. Hong-Lun and Z. Guang-Shi, "A study on nonlinear lateral stiffness of air spring for high speed railway," *Journal of the China Railway Society*, vol. 21, no. 5, pp. 30-33, 1999 (Chinese).
- [10] D. N. Wormley, D. P. Garg, and H. H. Richardson, "A comparative study of nonlinear and linear performance of vehicle air cushion suspensions using bond graph models," *Journal of Dynamic Systems, Measurement and Control*, vol. 94, no. 3, pp. 189-197, 1972.
- [11] C. M. Pappalardo, M. Wallin, A. A. Shabana, "A New ANCF/CRBF Fully Parametrized Plate Finite Element," *ASME Journal of Computational and Nonlinear Dynamics*, 12 (3), pp. 1-13, 2017.
- [12] S. Kulkarni, C. M. Pappalardo, A. A. Shabana, "Pantograph/Catenary Contact Formulations," *ASME Journal of Vibrations and Acoustics*, 139 (1), pp. 1-12, 2017.
- [13] C. M. Pappalardo, Z. Yu, X. Zhang, A. A. Shabana, "Rational ANCF Thin Plate Finite Element," *ASME Journal of Computational and Nonlinear Dynamics*, 11 (5), pp. 1-15, 2016.
- [14] S. Oman, M. Fajdiga, and M. Nagode, "Estimation of air-spring life based on accelerated experiments," *Materials and Design*, vol. 31, no. 8, pp. 3859-3868, 2010.
- [15] S.H. Choi and H.H. Cheung, "Virtual Prototyping for Rapid Product Development", in *Modeling and Simulation in Engineering, Prof. Catalin Alexandru (Ed.)*, InTech, 2012, DOI: 10.5772/25955.
- [16] J. Cecil, A. Kanchanapiboon, "Virtual engineering approaches in product and process design", in *The International Journal of Advanced Manufacturing Technology*, 2007, 31 (9): 846-856.
- [17] F. Renno, and S. Papa, "Direct Modeling Approach to Improve Virtual Prototyping and FEM Analyses of Bicycle Frames," *Engineering Letters*, vol. 23, no. 4, pp.333-341, 2015.
- [18] A. Lanzotti, F. Renno, M. Russo, R. Russo, M. Terzo, "Design and development of an automotive magnetorheological semi-active differential", *Mechatronics*, vol. 24, no. 5, pp. 426 - 435, 2014.
- [19] B. Bidanda, P.J., "Virtual Prototyping & Bio Manufacturing in Medical Applications", *Springer*, 2008. ISBN: 978-0-387-33429-5.
- [20] G. Di Gironimo, C. Labate, F. Renno, M. Siuko, A. Lanzotti, F. Crisanti, "An interactive design approach for nuclear fusion purposes: remote handling system for FAST divertor", *International Journal on Interactive Design and Manufacturing*, Vol. 8, Issue 1, Pages 55-65, February 2014.
- [21] G. Di Gironimo, C. Labate, F. Renno, G. Brolatti, F. Crescenzi, F. Crisanti, A. Lanzotti, F. Lucca, "Concept Design of Divertor Remote Handling System for the FAST Machine", *Fusion Engineering and Design*, Vol. 88, Issue 9-10, pp. 2052-2056, 2013.
- [22] G. Ramogida, G. Calabrò, V. Cocilovo, F. Crescenzi, F. Crisanti, A. Cucchiario, G. Di Gironimo, R. Fresa, V. Fusco, P. Martin, S. Mastrostefano, R. Mozzillo, F. Nuzzolese, F. Renno, C. Rita, F. Villone, G. Vlad, "Active toroidal field ripple compensation and MHD feedback control coils in FAST", *Fusion Engineering and Design* 88 (6-8), pp. 1156-1160, 2013.
- [23] G. Di Gironimo, D. Carfora, G. Esposito, C. Labate, R. Mozzillo, F. Renno, A. Lanzotti, M. Siuko, "Improving concept design of divertor support system for FAST tokamak using TRIZ theory and AHP approach", *Fusion Engineering and Design* 88 (11), pp. 3014-3020, 2013.
- [24] F. Crescenzi, S. Roccella, G. Brolatti, L. Cao, F. Crisanti, A. Cucchiario, G. Di Gironimo, C. Labate, F. Lucca, G. Maddaluno, G. Ramogida, F. Renno, "Vessel and In-Vessel Components Design Upgrade of the FAST machine", *Fusion Engineering and Design Volume 88 (9-10)*, pp. 2048-2051.
- [25] C. Labate, G. Di Gironimo, F. Renno, "Plasma facing components: a conceptual design strategy for the first wall in FAST tokamak". *Nuclear Fusion*, vol. 55, no. 11, DOI 10.1088/0029-5515/55/11/113013, 2015.
- [26] COMSOL Mutiphysics ® Guide, 2011.
- [27] ANSYS® Academic Research, Release 16.2, Help System, ANSYS, Inc.
- [28] J. Tu, G. H. Yeoh and C. Liu, "Computational Fluid Dynamics, A Practical Approach", *Elsevier* 2012, ISBN: 978-0-7506-8563-4.
- [29] A. Calabrese, G. Serino, S. Strano, M. Terzo, "Investigation of the Seismic Performances of an FRBs Base Isolated Steel Frame through Hybrid Testing", *Lecture notes in engineering and computer science: Proceedings of the World Congress on Engineering 2013, WCE 2013*, 3 - 5 July, 2013, London, U.K., pp. 1974 - 1978.
- [30] C. M. Chang, S. Strano, M. Terzo, "Modelling of Hysteresis in Vibration Control Systems by means of the Bouc-Wen Model," *Shock and Vibration*, vol. 2016, Article ID 3424191, 14 pages, 2016. doi:10.1155/2016/3424191.
- [31] S. Strano, M. Terzo, "A multi-purpose seismic test rig control via a sliding mode approach," *Structural Control and Health Monitoring*, 21 (8), pp. 1193 - 1207. DOI: 10.1002/stc.1641, 2014.
- [32] C. Abagnale, M. Cardone, P. Iodice, S. Strano, M. Terzo, G. Vorraro, "Theoretical and Experimental Evaluation of a Chain Strength Measurement System for Pedelecs," *Engineering Letters*, vol. 22, no. 3, pp. 102 - 108, 2014.
- [33] C. Abagnale, M. Cardone, P. Iodice, S. Strano, M. Terzo, G. Vorraro, "Power requirements and environmental impact of a pedelec. A case study based on real-life applications," *Environmental Impact Assessment Review*, 53 (7), pp. 1 - 7, 2015.
- [34] P. Iodice, C. Abagnale, M. Cardone, S. Strano, M. Terzo, G. Vorraro, "Performance Evaluation and Environmental Analysis of an Electrically Assisted Bicycle Under Real Driving Conditions," *Proc. of the ASME 12th Biennial Conference on Engineering Systems Design and Analysis (ESDA2014)*, ESDA2014-20438, Vol. 1, Copenhagen, Denmark, June 25 - 27, 2014.
- [35] S. Strano, M. Terzo, "A SDRE-based tracking control for a hydraulic actuation system," *Mechanical Systems and Signal Processing*, 60-61, pp. 715-726, 2015.